

# EFFECT OF HEAT TREATMENT ON THE MICROSTRUCTURES AND MECHANICAL PROPERTIES OF Al-4Cu-1.5Mg ALLOY

Emin Çadırılı 

Department of Physics, Faculty of Arts and Sciences, Niğde Ömer Halisdemir University, Niğde, Turkey

Hasan Kaya and Uğur Büyük

Department of Science Education, Education Faculty, Erciyes University, Kayseri, Turkey

Erkan Üstün

Department of Physics, Institute of Science, Niğde Ömer Halisdemir University, Niğde, Turkey

Mehmet Gündüz

Department of Physics, Faculty of Science, Erciyes University, Kayseri, Turkey

Copyright © 2021 American Foundry Society, corrected publication 2023  
<https://doi.org/10.1007/s40962-021-00667-8>

## Abstract

*In this work, the influence of different heat treatments (HT) processes on the microstructure and mechanical properties of cast Al-4Cu-1.5Mg alloy was investigated. To investigate the effect of HT, firstly Al-4Cu-1.5Mg samples were homogenized (solution treatment) at 500 °C/2h, water quenched at room temperature (RT) and then immediately exposed to an artificial aging process at 200 °C for various aging times of 1, 4, 8, 12, 16, 20 and 24 hours. Quantitative examinations after HT processes (solution treatment and aging) have shown that intermetallic phases (Al<sub>2</sub>Cu and Al<sub>2</sub>CuMg) were dissolved in the α-Al matrix phase and distributed along the grain boundary. Some mechanical properties (HVσ, σ<sub>TYS</sub>, σ<sub>UTS</sub>, σ<sub>CYS</sub>, E and δ) of a sufficient number of alloy samples exposed to different heat treatments were examined in detail. The data obtained show*

*that the conditions of solution treatment and aging in some conditions show superior mechanical properties than the sample in the form as-cast. The highest microhardness value (126 HV) was obtained for the α-Al matrix phase, which was subjected to solution treatment (only homogenization). After aging for 1h at 200 °C, the peak value of microhardness was achieved as 289.5 HV for intermetallic phases. The highest tensile strength (σ<sub>UTS</sub>) was obtained as 328 MPa for the sample which aged for 8h at 200 °C after solution treatment for 2h at 500 °C.*

**Keywords:** 2xxx alloy, solution treatment, artificial aging, microhardness, tensile strength, yield strength

## Introduction

Aluminum alloys are commonly used in the automotive industry as well as in the aviation and space industries due to their low density and desired physical properties.<sup>1-3</sup> 2xxx family of aluminum casting alloys are age hardenable, based on Al-Cu system, which offers high strength and hardness at ambient and elevated temperatures.<sup>1,2</sup> Copper is a strong precipitation reinforcement element in

aluminum alloy. The alloy containing up to 5.0 wt.% Cu shows very high strength and good toughness properties when exposed to artificial aging.<sup>4-9</sup> The addition of Cu and Mg to the aluminum plays an important role in the mechanism of significant dispersion strengthening, not only by solid solution reinforcement but also by forming θ (Al<sub>2</sub>Cu) and S (Al<sub>2</sub>CuMg) intermetallic (IMC) phases by heat treatment (HT).<sup>8</sup> To achieve improved mechanical properties, aluminum alloys are often exposed to different HT process.<sup>10-18</sup> Among these, one of the most interesting alloys is the Al-Cu-Mg ternary alloy.<sup>14</sup>

Received: 24 May 2021 / Accepted: 26 July 2021 / Published online: 12 August 2021

Reis et al.<sup>16</sup> have applied a series of HT on the 2024 alloy. In the first step, these researchers applied the solution treatment process at 495, 505 and 515 °C temperatures and then the artificial aging processes at two different temperatures such as 190 and 208 °C for different aging times. They reported that the highest hardness was achieved with a combination of 505 °C/2h solution treatment and 208 °C/2h aging process. In another study, Zhou et al.<sup>17</sup> investigated the low-temperature behavior of the 2024 alloy. These researchers have worked on 2024 alloy with cryogenic treatment (CT) with 2, 4, 6, 8 and 12-h variation at 77 K using liquid nitrogen. Findings showed that CT can increase the hardness of the material. Goodarzy et al.<sup>18</sup> applied the solution treatment at 500 °C for 0.7 h on the 2024 alloy and then performed the ECAP process with aging of 70 °C and 100 °C. The results showed that the aging process at 70 °C increased the hardness of the studied alloy.

Solution treatment is the first stage in which the alloy is heated between the solvus and solidus temperatures and held until all soluble phases dissolve and a uniform solid solution structure is produced.<sup>19</sup> The final stage in the precipitation hardening process is aging process, which allows controlled separation of the supersaturated solid solution and the formation of strengthening precipitates. Aging is the process of heating the supersaturated solid solution at a temperature below the solvus temperature to produce well-dispersed precipitates.<sup>19–23</sup>

Although there are a lot of studies and data in this area, the effect of an HT on compressive yield strength ( $\sigma_{CYS}$ ) and microhardness (HV) of intermetallic phases containing  $\theta$  and S has not been deeply investigated for Al–Cu–Mg alloy. The solution treatment process can be applied in one stage, two stages and sometimes three stages depending on the studied alloy composition and experimental conditions. In this study, Al–4Cu–1.5Mg (wt.%) alloy was preferred especially to observe the  $\theta$  and S phases resulting from precipitation hardening and the solution treatment was performed in one step at the maximum solubility limit. This composition equates to a low Cu/Mg ratio of 2.66. This Cu/Mg ratio is suitable for the formation of the precipitated phases. Therefore, the aim of this study is to determine which HT condition provides an improved mechanical property for the Al–4Cu–1.5Mg alloy. In the first stage, homogenization process was conducted on the studied alloy samples at a certain temperature and time. In the second stage, HT was completed by applying aging at a certain temperature and different aging times. After microstructural analysis of the samples and some mechanical testing, optimum values were found for microhardness (HV), ultimate tensile strength ( $\sigma_{UTS}$ ), tensile yield strength ( $\sigma_{TYS}$ ), compressive yield strength ( $\sigma_{CYS}$ ) and Young's modulus (E).

## Experimental Procedures

### Preparation of the Al–Cu–Mg Alloy

Al–4Cu–1.5Mg alloy (Figure 1) samples were prepared using high-purity (99.99%) Al, Cu and Mg metals (all compositions are given by weight unless otherwise specified). First, a sufficient amount of Al was placed in a graphite crucible (L: 180 mm, OD: 38 mm, ID: 25 mm) and melted in a vacuum furnace at set temperature of about 750 °C. After Al was completely melted, the required amount of solid Cu (4 wt.%) was inserted under the liquid Al surface. This liquid Al–Cu alloy was stirred three times at three-minute intervals, and then the required amount of Mg (1.5 wt.%) packed with pure thin Al foil was placed in a graphite cage with many holes (Figure 2a); it was then put under the surface of the liquid Al–Cu alloy in order to avoid Mg burning on the surface of the melt. After obtaining sufficient homogeneity and fluency, the molten alloy was poured through a funnel into seven alumina molds (100 mm long, 7 mm OD, 6 mm ID) placed in a casting furnace (Figure 2b and c). The lower and upper heaters of the casting furnace were kept at temperatures approximately 50 and 100 °C above the melting point of the alloy, respectively. To avoid air bubbles in the samples, each sample was stirred with a thin alumina stick. Then, an effective water cooling reservoir located at the bottom of the casting furnace was used to obtain homogeneously solidified samples. The sample preparation studies were repeated until the necessary numbers (27) of suitable samples were produced. Approximately 10 cm sections of both ends of the produced samples were cut and discarded. The purpose of taking this precaution is to avoid possible errors

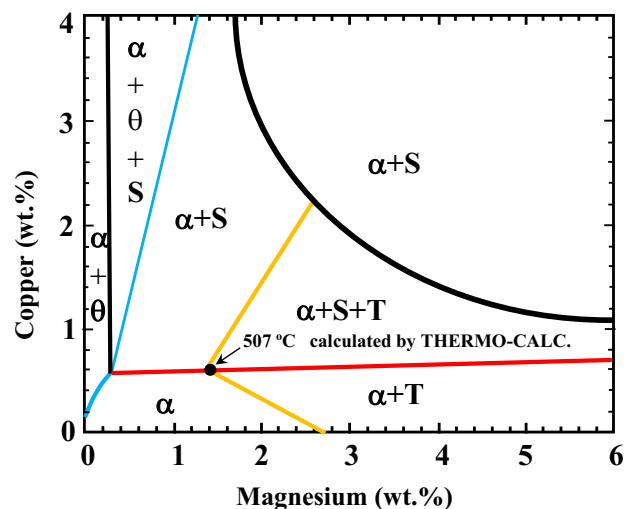


**Figure 1. Aluminum-rich corner of the Al–Cu–Mg phase diagram indicating the phases present as a function of composition<sup>20</sup> ( $\alpha$ :  $\alpha$ -Al phase,  $\theta$ :  $Al_2Cu$  phase, S:  $Al_2CuMg$ , T:  $Al_6CuMg_4$ )**

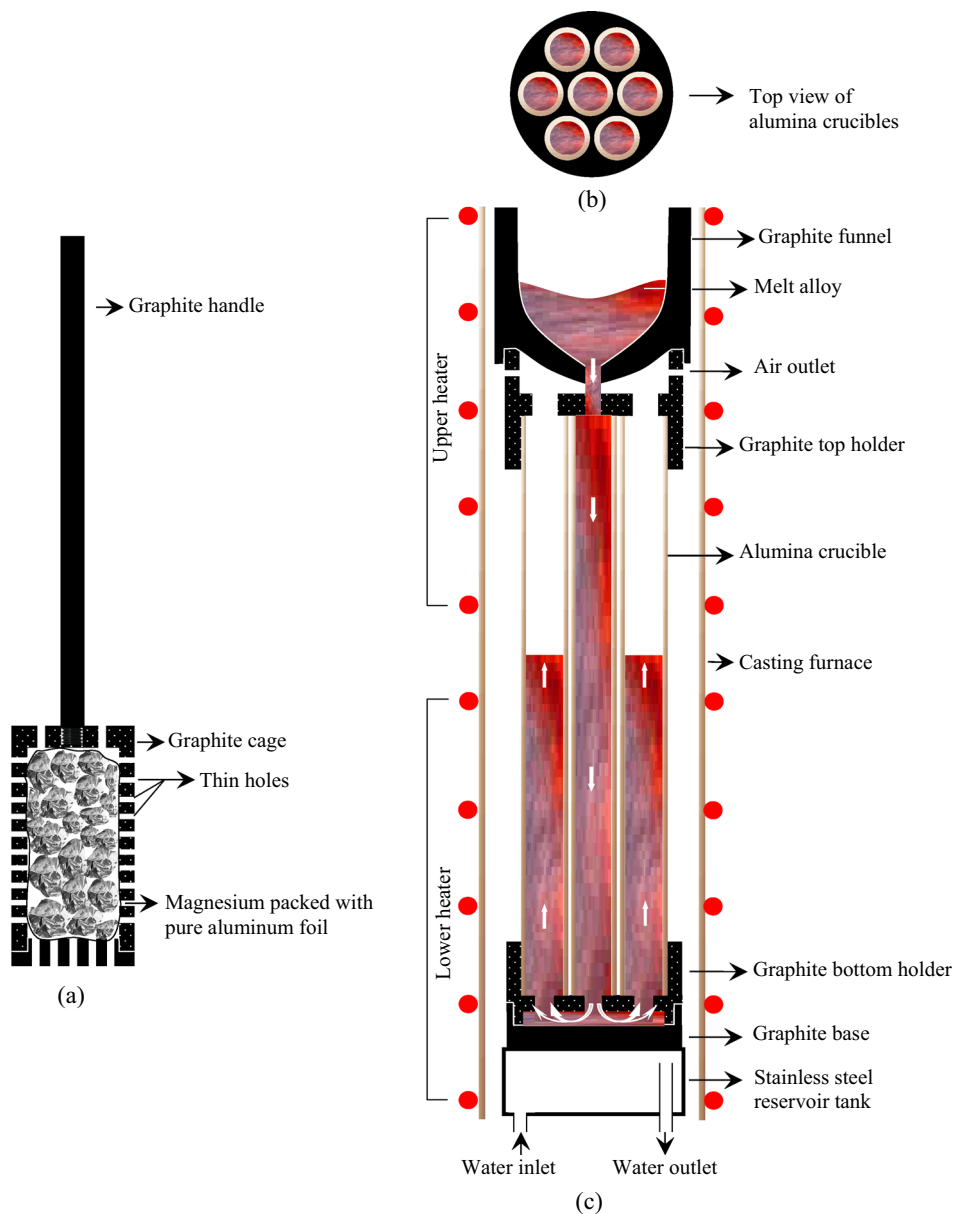


**Figure 2. (a) Graphite cage, (b) top view of alumina crucibles and (c) crucibles in the casting furnace**

during mechanical tests. The remaining 80-mm-long parts of the samples were prepared for the microstructure examination and mechanical tests (HV,  $\sigma_{TYS}$ ,  $\sigma_{UTS}$  and  $\sigma_{CYS}$ ).

### Heat Treatment

First, the required number (twenty-seven) of samples to produce microstructure, HV hardness, tensile strength ( $\sigma_{TYS}$ ,  $\sigma_{UTS}$ ) and compressive yield strength ( $\sigma_{CYS}$ ) testing were produced for each HT setting. In order to increase statistical reliability, three repetitions were run of each test and HT condition. The solution treatment (homogenization) and aging processes which are the HT steps to be applied in this study are given in schematically Figure 3.

To compare alloy samples to be heat treated with samples in as-cast form, three casting samples were kept in a refrigerator at  $-18\text{ }^{\circ}\text{C}$  without any HT and not allowing natural aging at room temperature (RT). The remaining twenty-four samples were exposed to  $500\text{ }^{\circ}\text{C}/2\text{h}$  solution treatment process (homogenization) and then quenched in water at RT (Figure 3a). After the solution treatment process, these twenty-four samples were divided into eight subgroups. One of these subgroups was preserved as an only homogenized group. In other words, it was not exposed to any aging treatment process. The remaining seven subgroups (three samples) were exposed to artificially aging process (T6) in different conditions (Figure 3b). As shown in Figure 3c, three test samples were allocated for each subgroup to increase the reliability of the data.

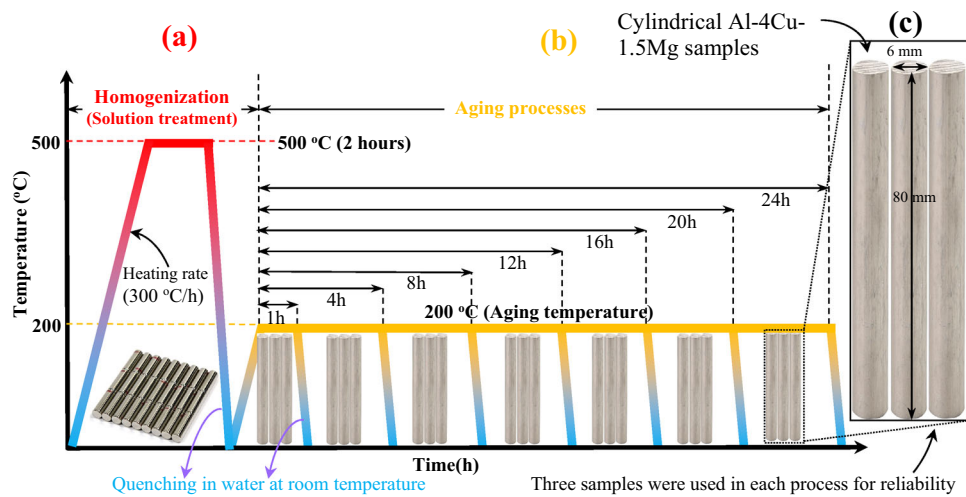


**Figure 3. (a) The homogenization (solution heat treatment) and (b) aging regimes for the Al-4Cu-1.5Mg alloy**

The HT (T6) was conducted in a muffle furnace. The maximum temperature at which this heat treatment can be carried out will depend on the content in Cu and Mg. According to the ternary phase diagram<sup>20</sup> given in Figure 1, the maximum solubility temperature is approximately 507 °C (eutectic temperature) and equilibrium phase structure is  $\alpha - \text{Al} + \theta + \text{S}$ . Therefore, the solution treatment temperature was set as 500 °C during the T6 heat treatment for the studied alloy. This process was optimized during preliminary research. Parameters of artificial aging applied to the alloys were developed based on common industry standards and literature studies. In the first step of the two-step HT process, the solution treatment process (500 °C/2 h) was carried out, and then, the process was completed by performing an artificial aging process in seven different conditions (1 h, 4 h, 8 h, 12 h, 16 h, 20 h and 24 h at 200 °C). For the solution treatment process, samples were heated (300 °C/h), from RT to solution processing temperature  $T$  (500 °C), kept at 500 °C for 2 hours and then quenched in water at RT to obtain a supersaturated solid solution. For the aging process, the solution-treated samples were heated (300 °C/h) again from RT to the aging temperature (200 °C) and held at this temperature for a certain time and then quenched in water at RT. The parameters applied in both solution treatment and aging process are given in Table 1. After the HT process, standard metallography process for all samples (without heat treated, only homogenized and homogenized+aged samples), microstructure analysis and mechanical tests (microhardness and tensile properties) were performed.

### Microstructure Characterization and Identification of Phases

All samples were taken with appropriate sections, first molded with cold molding material (epoxy resin). Then

**Table 1. Heat Treatment Processes of Studied Al-4Cu-1.5Mg Alloy Samples**

Number of sample	Process	Status
S1	Without heat treatment (WHT)	As-cast
S2	Only homogenization (OH)	500 °C/2 h
S3	H+artificial aging	500 °C/ 2 h+200 °C/1 h
S4	H+artificial aging	500 °C/ 2 h+200 °C/4 h
S5	H+artificial aging	500 °C/ 2 h+200 °C/8 h
S6	H+artificial aging	500 °C/ 2 h+200 °C/12 h
S7	H+artificial aging	500 °C/ 2 h+200 °C/16 h
S8	H+artificial aging	500 °C/ 2 h+200 °C/20 h
S9	H+artificial aging	500 °C/ 2 h+200 °C/24 h

these samples were prepared for examination by conventional mechanical grinding, and polishing processes followed by etching with Keller's reagent (2 mL HF, 3 mL HCl, 5 mL HNO<sub>3</sub> and 190 mL water) for 10 seconds. After that, the microstructures of all the samples were revealed and characterized using an inverted Nikon Eclipse MA 100 optical microscope and a Zeiss-Gemini 500 field effect scanning electron microscope (FESEM) equipped with an energy-dispersive X-ray (EDX) spectrometer as well as a computer-controlled image system. EDX analysis was performed to determine the composition of the matrix and

intermetallic compound (IMC) phases in samples of studied alloy at 20 keV using the X-ray lines. Besides, X-ray diffraction (XRD) analysis was conducted to confirm the accuracy of the data obtained from the EDX analysis. XRD measurements were conducted with a diffractometer (Rigaku Ultima IV) using Cu-K $\alpha$  radiation ( $k = 1.5405 \text{ \AA}$ ) at an accelerating voltage of 40 kV. The diffracted beam was scanned in steps by  $0.01^\circ$  across a  $2\theta$  range of  $20\text{--}90^\circ$ . The EDX and XRD analysis results and related comments are given in detail in the next section.

### Measurement of the Microhardness (HV)

Microhardness measurements were conducted at room temperature with a *Future-Tech FM-700 model* microhardness test apparatus. In these measurements, 300 g load was applied to the polished sample surface for 10s. Approximately 20–25 measurements were taken for each sample section. Mean values were calculated from these microhardness values. Some errors inevitably occurred during the microhardness measurements. These errors are caused by factors such as surface quality of the sample, inhomogeneous phase distributions in the microstructure and uncertainty of the traces. In this case, a measurement error may occur, since the sharpness cannot be achieved sufficiently during the measurement of the diagonal lengths of the trace formed on the surface of sample. The percentage of error in hardness measurements is reasonable (6%) and is within the systematic measurement error limits of the hardness measurement device.

### Measurement of Tensile Yield Strength ( $\sigma_{\text{TYS}}$ ), Ultimate Tensile Strength ( $\sigma_{\text{UTS}}$ ) and Compressive Yield Strength ( $\sigma_{\text{CYS}}$ )

The measurements of tensile yield strength and ultimate tensile strength of the samples were performed with a *Shimadzu AG-XD* testing apparatus with a strain rate ( $10^{-3} \text{ s}^{-1}$ ) at RT. The samples (as-cast and heat-treated samples) in cylindrical form for tensile strength were prepared to be 6 mm in diameter and 60 mm in length (Figure 3c). To increase the reliability of tensile tests, the tests were repeated three times for each regime and the mean value was taken. Similarly, cylindrical samples with a diameter of 6 mm and a length of 8 mm were used in compressive strength tests. For the test to be reliable, the deformation rate was chosen as 1 mm/min. Also, compression tests were repeated three times like tensile tests and the mean value was taken. It has been found that the experimental error was about 5% for both tensile and compressive tests.

## Results and Discussion

### Heat Treatment

Both optical (OM) and SEM images of the as-cast sample are shown in Figure 4. It can be seen that the microstructure of the as-cast sample consists of  $\alpha$ -Al (matrix phase) and second phases. As-cast microstructures contain both coarsened dendritic  $\alpha$ -Al solid solution and nonequilibrium second phases. These secondary phases are intermetallic phases that mainly precipitate on grain boundaries and interdendritic regions during solidification. For this reason, the distribution of the  $\alpha$ -Al solid solution and IMC phases during solidification is uneven and composition segregation usually occurs too. In addition, unstable distribution of temperature, impurity, metallic or nonmetallic inclusion and so on can also result in inhomogeneous microstructure.<sup>25</sup> However, the as-cast microstructures are unstable and can be improved by HT (homogenization and aging).<sup>25</sup> The most important point to be considered in the solution treatment process is that the process temperature should not exceed the lowest melting point of any phase in the sample.<sup>26</sup> During the HT process, dendritic segregation will gradually decrease and the unstable phases will turn into the stable phases. Optimum HT parameters should be found by providing different conditions. Many scientists have worked on the HT process of 2xxx alloys for decades, and they have proposed some optimum parameters for advantageous HT.<sup>7,9–11,14,17,18,20,27–29</sup>

### Microstructure Characterization

The mechanical properties mainly depend on the microstructures of the material; therefore, OM and SEM analyses were performed to characterize microstructures, and chemical composition analyses of the phases were determined with EDX and XRD analysis. As can be seen from Figure 5, chemical results of the heat-treated (500 °C/2h+200 °C/1h) alloy (S3) are given in the EDX spectrum. The microstructures observed in the sample (S3) consisted mainly of larger  $\alpha$ -Al grains (gray region) and IMC phases ( $\theta$  and  $S$ ) in the grain boundaries (dark region) in  $\alpha$ -Al matrix. According to the EDX, although the composition ratios (94.62 Al, 4.15 Cu and 1.23 Mg wt.%) in the gray region are close to the nominal composition, the composition ratios (43.02 Al, 47.21 Cu and 9.77 Mg wt.%) in the dark region are very rich in Cu and Mg and formed intermetallic phases. The constituent phases of the sample (S3) were identified with XRD analysis. The XRD pattern of the heat-treated alloy (S3) is shown in Figure 6. As indicated, the presence of  $\alpha$ -Al (dominant phase),  $\text{Al}_2\text{Cu}$  and  $\text{Al}_2\text{CuMg}$  is confirmed due to the high number of peaks corresponding to these matrix phase and IMC phases, respectively. Both EDX analysis (Figure 5) and XRD pattern (Figure 6) strongly indicate that only three phases

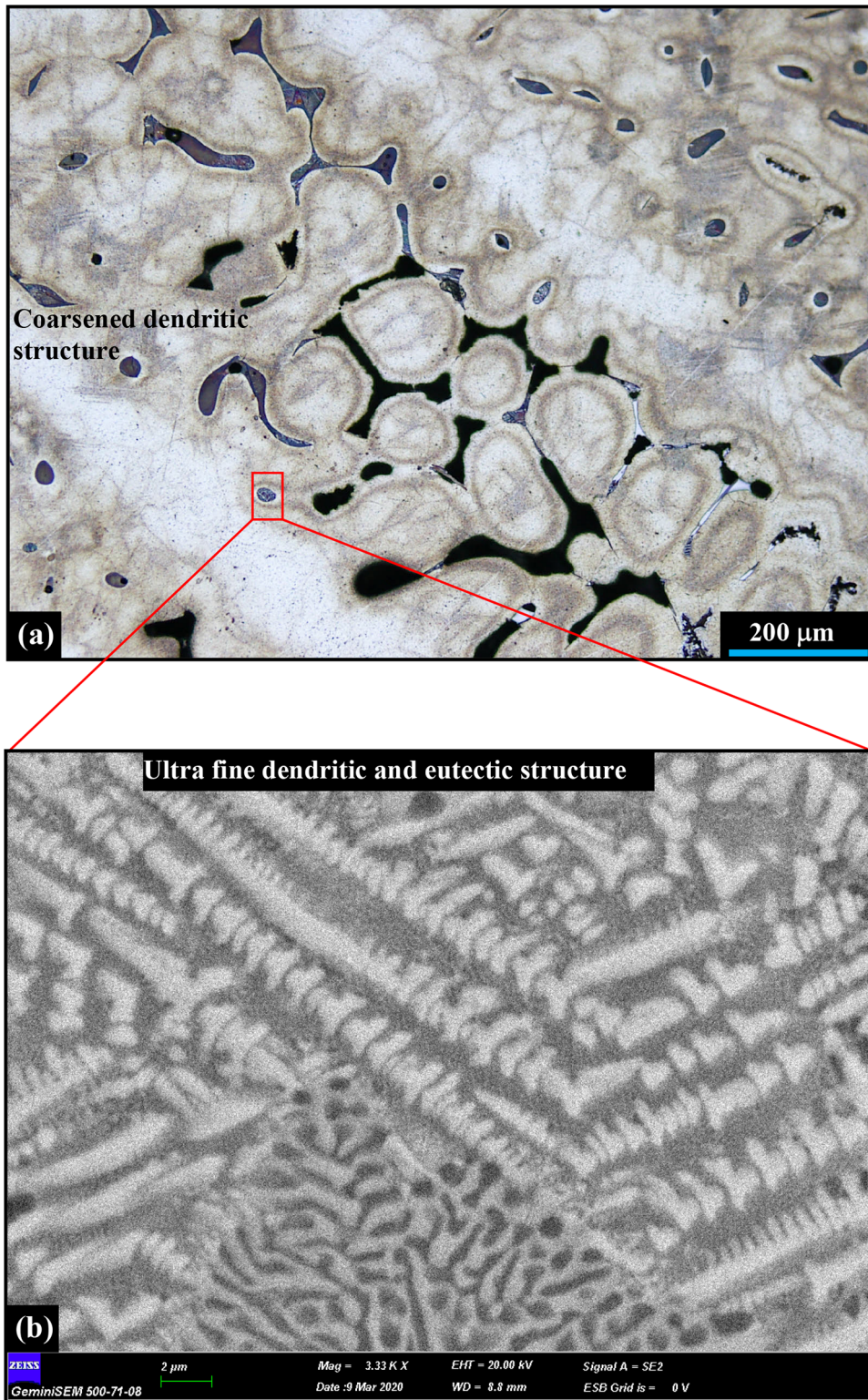
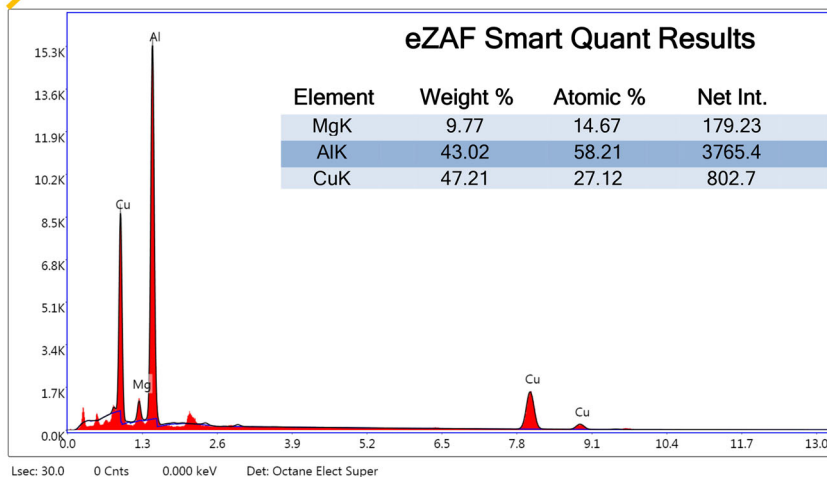
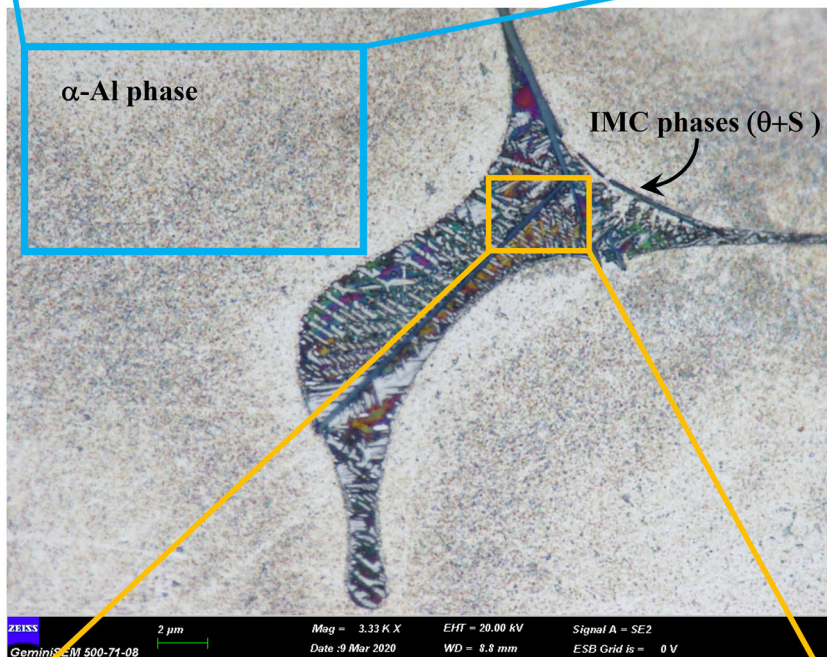
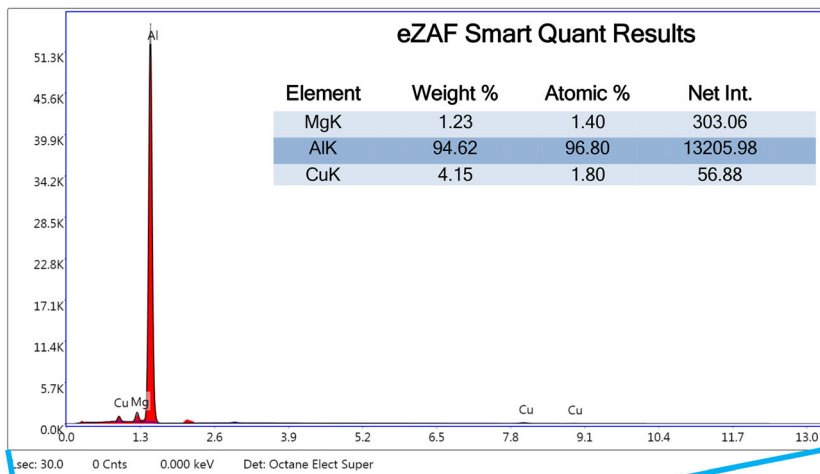


**Figure 4. Optical and SEM micrographs of as-cast Al-4Cu-1.5Mg alloy (S1)**

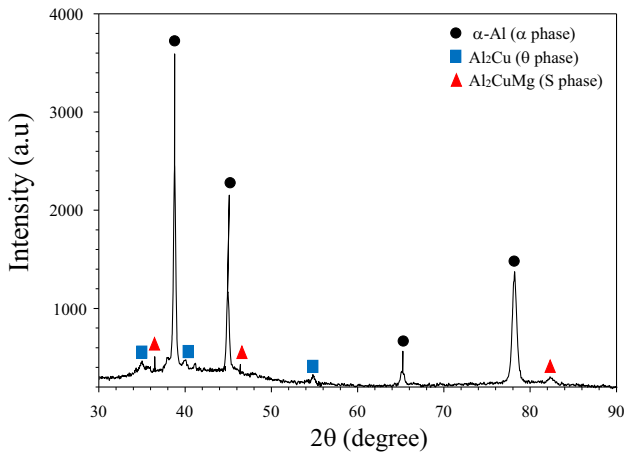
( $\alpha$ -Al, Al<sub>2</sub>Cu and Al<sub>2</sub>CuMg) are present in the microstructure of the sample (S3).

Figure 7 shows the TEM micrograph for the S5 sample aged (8h at 200 °C) after being homogenized (2h at 500 °C). In this micrograph, Al<sub>2</sub>CuMg (S phase) and

Al<sub>2</sub>Cu ( $\theta$  phase) precipitates (IMCs) have formed, which were defined as polyhedral-shaped and spherical particles, respectively. As can be seen from this figure again, the precipitates have different shapes: Some (the dark bigger ones) were polyhedral-shaped Al<sub>2</sub>CuMg particles and some spherical-shaped Al<sub>2</sub>Cu particles (the open smaller ones).



**Figure 5. EDX spectrum of the heat-treated sample (S3) of the Al-4Cu-1.5Mg alloy**



**Figure 6. XRD pattern obtained from the heat-treated sample (S3) of the Al-4Cu-1.5Mg alloy**

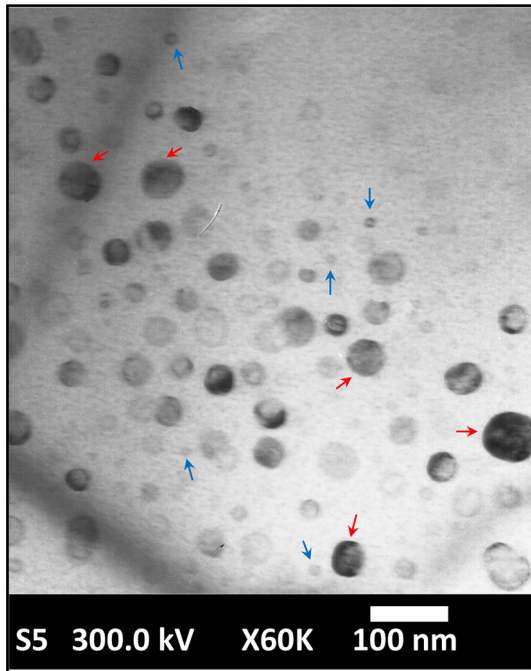


**Figure 7. TEM micrograph (bright-field image) of Al<sub>2</sub>CuMg (S phase, red arrows) and Al<sub>2</sub>Cu (θ phase, blue arrows) precipitates in the S5 sample aged with the aging regime (8 h at 200 °C) after the homogenization (2 h at 500 °C)**

The size of Al<sub>2</sub>CuMg particles is about 30–60 nm, while the size of Al<sub>2</sub>Cu particles is 10–35 nm and dispersed in the eutectic phase and at the grain boundaries.

Typical OM microstructures of the as-cast (WHT) and heat-treated Al-4Cu-1.5Mg alloy are shown in Figure. 8. Figures 4a and 8a show the coarsened dendritic structure of the as-cast of the studied alloy (S1). However, coarsening dendritic structures have disappeared in the structures of heat-treated samples (S2–S9) and grain boundaries have been further thinned (Figure 8b–i). The solution-treated

sample or only homogenized (OH) sample (S2 in Figure 8b) and aged samples (S3–S9) in Figure 8c–i) originate from the same as-cast Al-4Cu-1.5Mg alloy. Since the aged alloy samples were exposed to the same solution treatment regime (500 °C/2h), it can be considered that the aged alloy samples have the same original microstructure before aging. For this reason, the difference in the microstructures of artificially aged alloy samples is caused by the different aging regimes used in this study. Since aging is a precipitation process, the microstructure difference between artificially aged alloy samples is closely related to the type, size and number of precipitates.

## Microhardness

Microhardness values of all samples were measured both on matrix phases (α-Al) and on IMC phases (Al<sub>2</sub>Cu and Al<sub>2</sub>CuMg), usually clustered at grain boundaries. Microhardness values obtained for IMC phases were more than twice compared to those obtained for matrix phase. Figure 9 illustrates the HV values of the samples. Average HV value of the matrix phases of as-cast (S1) sample without HT is found to be 61 HV. However, the average HV value for the IMC phases of the same sample (S1) was obtained as 120.1 HV. Peak hardness values for matrix and IMC phases are obtained as 126.2 HV (500 °C/2 h (S2)) and 289.5 HV (500 °C/2h + 200 °C/1 h (S3)), respectively. Peak HV value (126.2 HV) for matrix phase is in very good agreement with values 119 HV, 127 HV and 129 HV obtained by Zamani et al.<sup>28</sup> at 190 °C/4h aging process after solution treatment (495 °C/5 h), Feng et al.<sup>29</sup> at 190 °C/12 h aging process after solution treatment (500 °C/3h) and Yamanoglu et al.<sup>30</sup> at 200 °C/6 h aging process after solution treatment (540 °C/6 h), respectively, for Al-Mn-Cu alloys. The peak hardness value (289.5 HV) obtained for the IMC phase is also very close to the value (300 HV) obtained by Petrova et al.<sup>31</sup> at two-stage aging (120 °C with holding for 1.5 h and 160 °C for 6h) by the T6I6 regime after solution treatment at a temperature of 500 °C for 16 h. As can be understood from these comparisons, the optimum HT condition (S3), which requires a shorter time, has been determined for the maximum microhardness value in the Al-4Cu-1.5Mg alloy.

## Tensile Yield Strength and Ultimate Tensile Strength

Typical strength-strain curves of Al-4Cu-1.5Mg samples are shown in Figure 10. The tensile yield strength ( $\sigma_{TYS}$ ) and elongation ( $\delta$ ) values of the samples are defined from the curves in Figure 10. The yield point is the point on a strength-strain curve that indicates the limit of elastic behavior and the beginning of plastic behavior.  $\sigma_{TYS}$  values are shown in Figure 11. As can be seen from Figures 10 and 11, while the highest  $\sigma_{TYS}$  value (268.3 MPa) was in



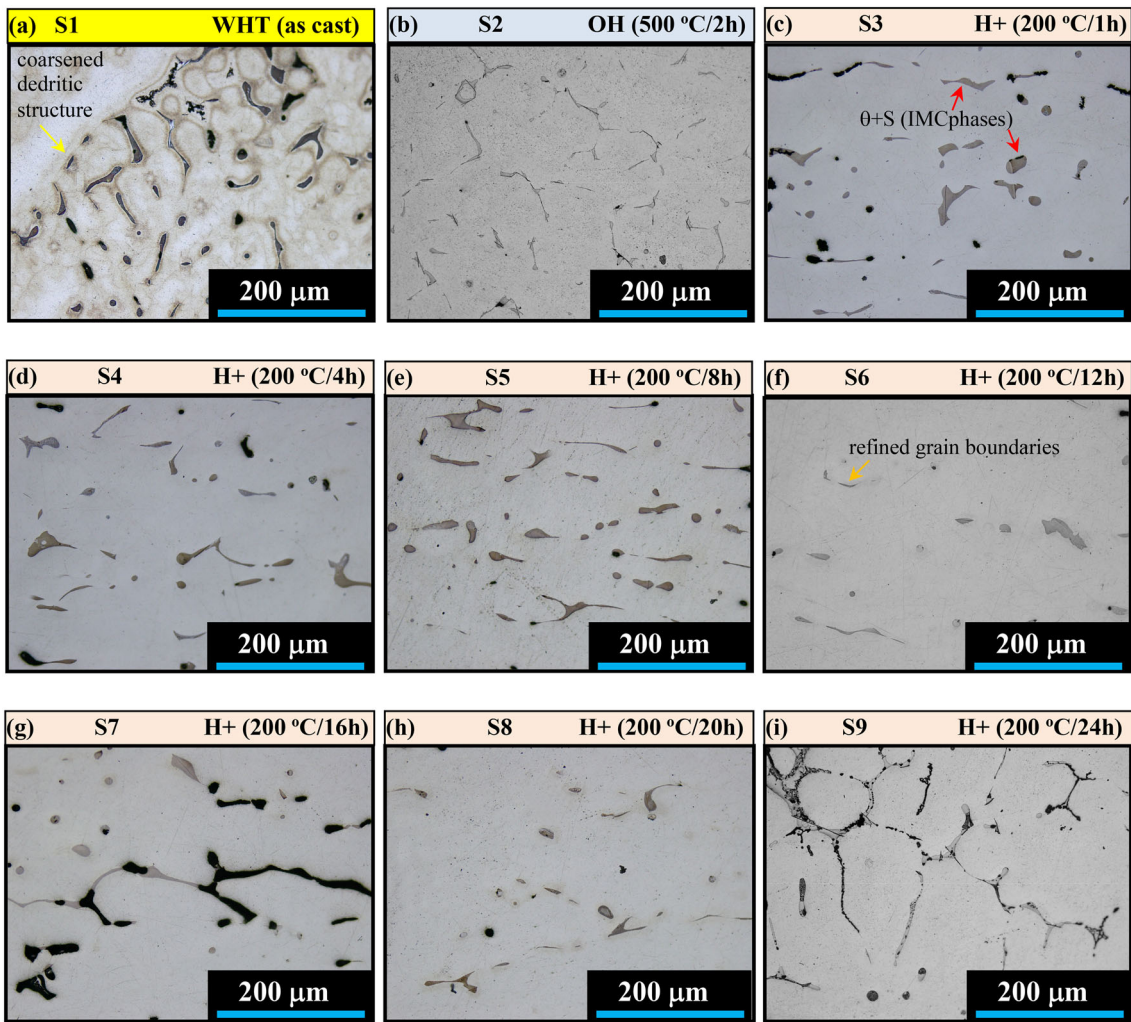


**Figure 8.** Optical micrographs of the as-cast (WHT) and heat treated Al-4Cu-1.5Mg alloy (a) as-cast sample (S1), (b) only homogenized sample (or solution treatment) (S2) and (c-i) aged samples at different times after homogenization (S3-S9)

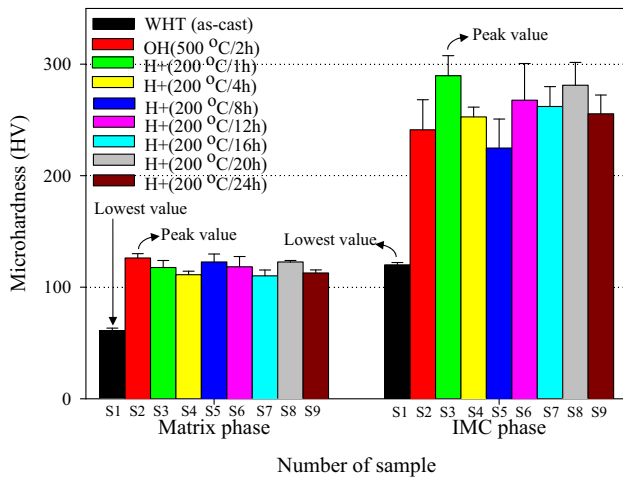


**Figure 9.** The effect of solution treatment and aging treatment on the microhardness

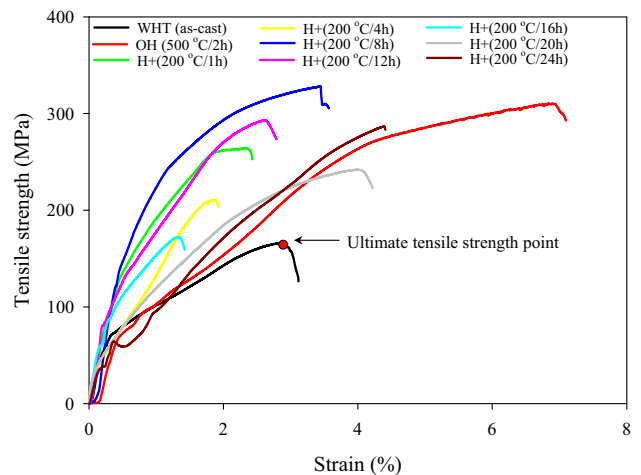


**Figure 10.** Typical tensile strength-strain curves of heat-treated Al-4Cu-1.5Mg alloys

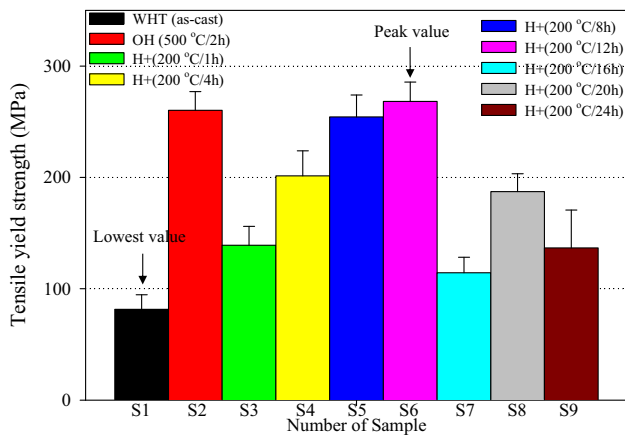


**Figure 11. The effect of solution treatment and aging treatment on the tensile yield strength**

the S6 sample (500 °C/2 h+ 200 °C/12 h), the highest  $\delta$  value (3.89%) was determined in the S2 sample (500 °C/2 h). In addition, the minimum  $\sigma_{TYS}$  (81.51 MPa) and  $\delta$  (0.55%) values were obtained for the as-cast sample (S1) without any heat treatment. Ultimate tensile strength ( $\sigma_{UTS}$ ) and elongation ( $\delta$ ) values were determined from the curves in this graph (Figure 10) again. Both the  $\sigma_{UTS}$  and  $\delta$  of some samples (S2, S5, S8 and S9) increased compared to the as-cast sample (S1). However, in some samples (S3, S4, S6 and S7), while the  $\sigma_{UTS}$  increased, the  $\delta$  decreased compared to the as-cast sample (S1). As can be seen from the curves given in Figure 10, the  $\delta$  of the as-cast sample (S1) without any heat treatment is 2.8%. The ductility of the material in terms of the elongation increased significantly in comparison with the as-cast sample (S1) and reached 6.9% in the S2 sample after the solution treatment process (500 °C/2 h). If the S7 sample is compared with the S1 sample, it will be observed that there is a significant decrease (55%) in the amount of  $\delta$  (1.3%) while a small increase (4%) in  $\sigma_{UTS}$  (172.5). The values of the  $\sigma_{UTS}$  are shown in Figure 12. The lowest value was obtained as 166 MPa for the as-cast sample (S1). This value reached

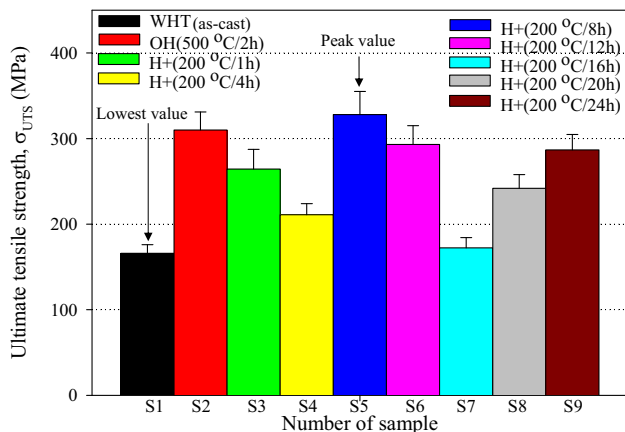


**Figure 12. The effect of solution treatment and aging treatment on the ultimate tensile strength**

310 MPa in the solution treatment process (S2) as shown in Figure 12. In different aging regimes applied after the solution treatment process, the others were obtained below 310 MPa except for one aging regime (S5). Peak  $\sigma_{UTS}$  value was obtained as 328 MPa for this aging regime (S5) and 97% improvement was achieved compared to the tensile value of the as-cast sample (S1). If we compare the optimum HT conditions, we have determined in terms of maximum microhardness and maximum tensile strength, an aging time of 1 hour (S3) is sufficient to reach the maximum microhardness value, while an aging time of 8 hours (S5) is required for maximum tensile strength.

The peak  $\sigma_{TYS}$  value (268.3 MPa) obtained by us is fairly close to value 256.4 MPa obtained by Elgallad et al.<sup>7</sup> under similar aging conditions (220 °C/6h) for Al–2.1Cu–0.4Mg–0.8Fe–0.8Mn alloy. The peak  $\sigma_{UTS}$  value (328 MPa) is in good agreement with value 330 MPa obtained by Samuel et al.<sup>32</sup> at 200 °C/5 h aging process after solution treatment (495 °C/8h) for 220 Al–2Cu-based alloy. Also, peak  $\sigma_{UTS}$  value is lower than values 385 MPa and 367 MPa obtained by Feng et al.<sup>29</sup> at 190 °C/12 h aging process after solution treatment (500 °C/3 h) for Al–4Cu–1.3Mg alloy and Zhao et al.<sup>33</sup> at 180 °C/6 h aging process after solution treatment (495 °C/2 h) for Al–4.5Cu–1.5Mg alloy, respectively. This improvement in tensile strength is due to precipitation hardening. Similar behaviors were reported by Petrova et al.<sup>31</sup>, Li et al.<sup>34</sup>, Zhang et al.<sup>35</sup> and Gu et al.<sup>36</sup> for 2xxx alloys with different compositions. It can be said that the strengthening mechanism for the studied alloy is due to the precipitation hardening. In some studies, it was emphasized that the dislocation movement is effective in the precipitate formation process.<sup>37–39</sup>

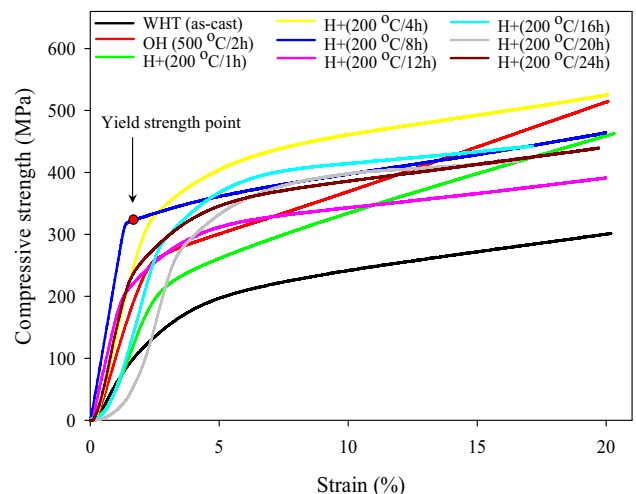


**Figure 13. Typical compressive strength–strain curves of heat-treated Al–4Cu–1.5Mg alloys**

## Compressive Strength

Compressive strength–strain curves for Al–4Cu1.5Mg samples are shown in Figure 13. Compressive yield strength values ( $\sigma_{CYS}$ ) were determined from strength–strain curves (yield strength point indicated by red dot). The values of the  $\sigma_{CYS}$  under different heat treatment processes are shown in Figure 14. The  $\sigma_{CYS}$  value of the as-cast sample (S1) is found to be 187.1 MPa. This value is the lowest value for  $\sigma_{CYS}$ , but this value improved in aging processes applied for different times. The  $\sigma_{CYS}$  of the sample (S4) reached to 337.3 MPa (peak value) with the aging process (200 °C/4h) applied after the solution treatment (500 °C/2h). The maximum gain of 150.2 MPa (80.2%) of the S4 sample was obtained. As can be understood from these results, unlike other mechanical properties (HV,  $\sigma_{UTS}$ ), the optimum HT condition for maximum compressive yield strength was the 4 hours aging process (S4) applied after the solution treatment. Peak value (337.3 MPa) of  $\sigma_{CYS}$  obtained in this study is in very good agreement with values 310 MPa, 300 MPa and 331 MPa obtained by Feng et al.<sup>29</sup> at 190 °C/12h aging process after solution treatment (500 °C/3 h) for Al–4Cu–1.3Mg alloy, Samuel et al.<sup>32</sup> at 200 °C/5h aging process after solution treatment (495 °C/8h) for 220 Al–2Cu-based alloy and Zhan et al.<sup>40</sup> at 160 °C/12h aging process for Al–4.26Cu–1.36Mg alloy, respectively.

## Young Modulus

The Young modulus ( $E=\sigma/\epsilon$ ) can be defined as the slope of the linear part of the stress–strain curve that occurs when a material is subjected to tensile testing. Young modulus values defined from strength–strain curves in Figure 10 are given in Figure 15. The lowest value was obtained as 35.7 GPa for the S9 sample. The Young's modulus of the sample (S4) reached 100.3 GPa (peak value) with the aging process (200 °C/4h) applied after the solution treatment

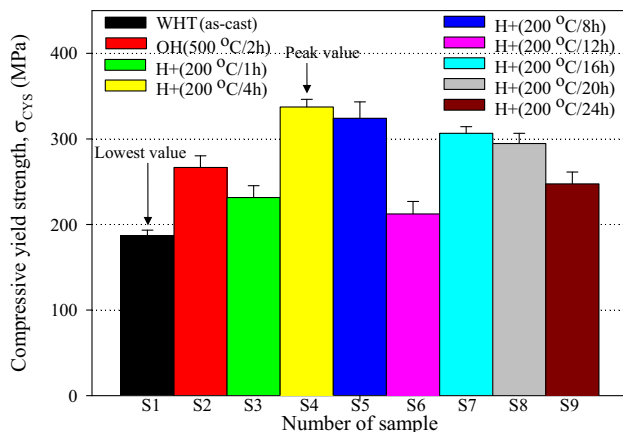


**Figure 14. The effect of solution treatment and aging treatment on the compressive yield strength**

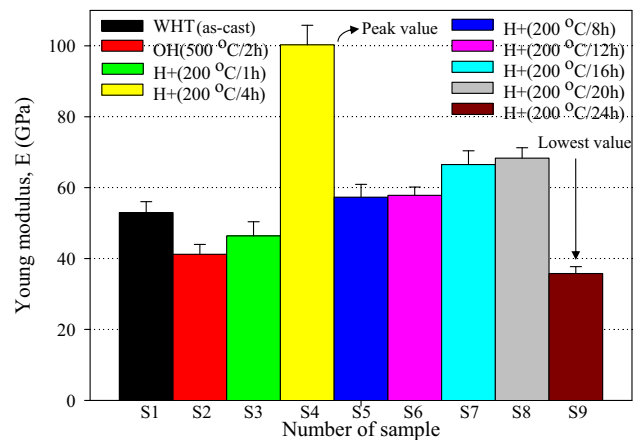


**Figure 15. Young modulus of heat-treated Al–4Cu–1.5Mg alloys**

**Table 2. Heat Treatments Where Mechanical Properties Reach Peak Value**

Mechanical properties	Peak values	Process (number of sample)
Microhardness of matrix phase (HV)	126.2 HV	500 °C/2 h (S2)
Microhardness of IMC phase (HV)	289.5 HV	500 °C/ 2 h+200 °C/1 h (S3)
Tensile yield strength ( $\sigma_{TYS}$ )	268.3 MPa	500 °C/ 2 h+200 °C/12 h (S6)
Ultimate tensile strength ( $\sigma_{UTS}$ )	328.0 MPa	500 °C/ 2 h+200 °C/8 h (S5)
Elongation ( $\delta$ )	6.9%	500 °C/2 h (S2)
Compressive yield strength ( $\sigma_{CYS}$ )	337.3 MPa	500 °C/ 2 h+200 °C/4 h (S4)
Young modulus (E)	100.3 GPa	500 °C/ 2 h+200 °C/4 h (S4)

(500 °C/2h). Peak value of E (100.3 GPa) is close to with values 109.3 GPa and 100.1 GPa calculated by Zhang et al.<sup>41</sup> for Al–Cu–Mg alloy and obtained by Kaczmarek et al.<sup>42</sup> after treatment by regime T616 for the matrix phase of 2024 alloy, respectively. The peak values of the mechanical properties detected after HT are given in Table 2. Changes in elastic constants of multicomponent materials can be quite complex. It is quite natural to have this complexity. There are many factors that affect the heat treatment processes applied after solidification such as microstructure (size, shape and composition of the different constituent phases), presence of precipitates (composition,

distribution, size of the particles) and interactions between dislocations.<sup>43</sup>

## Conclusions

Al-4Cu-1.5Mg alloy was produced using the vacuum furnace and the casting furnace. Microstructure and mechanical properties of cast (S1) and heat-treated samples (S2-S9) were investigated. The key findings are drawn as follows:

1. The microstructure of the cast sample (S1) consisted of  $\alpha$ -Al (coarse dendritic structure) and second phases. However, coarsening dendritic structures have disappeared in the structures of heat-treated samples (S2-S9) and grain boundaries have been further refined.
2. Substantial improvements in the microhardness of the Al-4Cu-1.5 Mg alloy were attained at different aging processes (200 °C/1 h-24 h) after solution treatment (500 °C/2 h). Peak hardness values for matrix and IMC phases are obtained as 126.2 HV (500 °C/2 h (S2)) and 289.5 HV (500 °C/2 h + 200 °C/1 h (S3)), respectively.
3. The peak  $\sigma_{TYS}$  value was obtained as 268.3 MPa for this aging regime (S6). The peak elongation value in the S2 sample reached 3.89%.
4. The peak  $\sigma_{UTS}$  value was obtained as 328 MPa for this aging regime (S5) and 97% improvement was achieved compared to the tensile value of the as-cast sample (S1). The highest average  $\sigma_{UTS}$  about 328 MPa was obtained for the S5 samples. The peak elongation value in the S2 sample reached 6.9%.
5. The compressive yield strength of the S4 sample reached 337.3 MPa with the aging process (200 °C/4 h) applied after the solution treatment (500 °C/2 h). The maximum gain of the S4 sample was calculated to be about 80.2%.
6. The Young modulus of S4 sample reached 100.3 GPa with the aging process (200°C/4 h) applied after the solution treatment (500 °C/2 h).

## Acknowledgements

This work was supported by the Erciyes University Scientific Research Project Unit Contract No: FBA-2019-9155. The authors are grateful for the financial supports for Erciyes University Scientific Research Project Unit.

## REFERENCES

1. D. Bakavos, P.B. Prangnell, B. Bes, F. Eberl, The effect of silver on microstructural evolution in two

- 2xxx series Al-alloys with a high Cu: Mg ratio during ageing to a T8 temper. *Mater. Sci. Eng. A* **491**, 214-223 (2008). <https://doi.org/10.1016/j.msea.2008.03.014>
2. B.T. Sofyan, K. Raviprasad, S.P. Ringer, Effects of microalloying with Cd and Ag on the precipitation process of Al-4Cu-0.3Mg (wt.%) alloy at 200 °C. *Micron* **32**, 851-856 (2001). [https://doi.org/10.1016/S0968-4328\(00\)00093-7](https://doi.org/10.1016/S0968-4328(00)00093-7)
3. P. Ashtari, G. Birsan, A. Khalaf, S. Shankar, Controlled diffusion solidification of 2024, 6082 and 7075 Al alloys via tilt-pour casting process. *Inter. J. Metalcast.* **5**, 43-64 (2011). <https://doi.org/10.1007/BF03355471>
4. M. Eddahbi, J.A. Jimenez, O.A. Ruano, Microstructure and creep behaviour of an Osprey processed and extruded Al-Cu-Mg-Ti-Ag alloy. *J. Alloys Compd.* **433**, 97-107 (2007). <https://doi.org/10.1016/j.jallcom.2006.06.031>
5. R.N. Lumley, I.J. Polmear, The effect of long term creep exposure on the microstructure and properties of an underaged Al-Cu-Mg-Ag alloy. *Scripta Mater.* **50**, 1227-1231 (2004). <https://doi.org/10.1016/j.scriptamat.2004.02.001>
6. A. Kordijazi, D. Weiss, S. Das, S. Behera, H.M. Roshan, P. Rohatgi, Effect of solidification time on microstructure, wettability, and corrosion properties of A205-T7 aluminum alloys. *Inter. J. Metalcast.* **15**, 2-12 (2021). <https://doi.org/10.1007/s40962-020-00457-8>
7. E. Elgallad, F. Samuel, A. Samuel, H. Doty, Development of new Al-Cu based alloys aimed at improving the machinability of automotive castings. *Inter. J. Metalcast.* **3**, 29-41 (2009). <https://doi.org/10.1007/BF03355446>
8. M.V. Glazoff, V.S. Zolotarevsky, N.A. Belov, *Casting Aluminum Alloys*, 1st edn. (Elsevier, Moscow, 2007)
9. J. Vietz, I. Polmear, The influence of small additions of silver on the ageing of aluminium alloys-observations on Al-Cu-Mg alloys. *J. Inst. Met.* **94**, 410-419 (1966)
10. N. Ünlü, B.M. Gable, G.J. Shiflet, E.A. Jr Starke, The effect of cold work on the precipitation of  $\Omega$  and  $\theta$  in a ternary Al-Cu-Mg alloy. *Metall. Mater. Trans. A.* **34**, 2757-2769 (2003). <https://doi.org/10.1007/s11661-003-0177-y>
11. M. Song, Y. He, D. Xiao, B. Huang, Effect of thermomechanical treatment on the mechanical properties of an Al-Cu-Mg alloy. *Mater. Design.* **30**, 857-861 (2009). <https://doi.org/10.1016/j.matdes.2008.05.053>
12. E. Cadırlı, H. Tecer, M. Şahin, E. Yılmaz, T. Kırındı, M. Gündüz, Effect of heat treatments on the microhardness and tensile strength of Al-0.25 wt% Zr alloy. *J. Alloys Compd.* **632**, 229-237 (2015). <https://doi.org/10.1016/j.jallcom.2015.01.193>
13. E. Acer, E. Çadırlı, H. Erol, T. Kırındı, M. Gündüz, Effect of heat treatment on the microstructures and

- mechanical properties of Al–5.5Zn–2.5Mg alloy. *Mat. Sci. Eng. A* **662**, 144–156 (2016). <https://doi.org/10.1016/j.msea.2016.03.073>
14. K.S. Al-Rubaie, M.A. Del Grande, D.N. Travessa, K.R. Cardoso, Effect of pre-strain on the fatigue life of 7050–T7451 aluminium alloy. *Mater. Sci. Eng. A* **464**, 141–150 (2007). <https://doi.org/10.1016/j.msea.2007.02.024>
  15. A. Polat, M. Avsar, F. Öztürk, Effects of the artificial-aging temperature and time on the mechanical properties and springback behavior of AA6061. *Mater. Technol.* **49**, 487–493 (2015). <https://doi.org/10.17222/mit.2013.154>
  16. D.A.P. Reis, A.A. Couto, N.I. Domingues Jr, A.C.O. Hirschmann, S. Zepka, C.M. Neto, 2012, Effect of artificial aging on the mechanical properties of an aerospace aluminum alloy 2024. *Defect and Diffusion Forum Vols. 326–328*, Trans Tech Publications, Switzerland (2012).
  17. J. Zhou, S. Xu, S. Huang, X. Meng, J. Sheng, H. Zhang, J. Li, Y. Sun, E.A. Boateng, Tensile properties and microstructures of a 2024–T351 aluminum alloy subjected to cryogenic treatment. *Metals* **6**, 279 (2016). <https://doi.org/10.3390/met6110279>
  18. M.H. Goodarzy, H. Arabi, M.A. Boutorabi, S.H. Seyedein, S.H.H. Najafabadi, The effects of room temperature ECAP and subsequent aging on mechanical properties of 2024 Al alloy. *J. Alloys Compd.* **585**, 753–759 (2014). <https://doi.org/10.1016/j.jallcom.2013.09.202>
  19. L. Wu, W.G. Ferguson, Modelling of precipitation hardening in casting aluminium alloys, aluminium alloys, theory and applications, T. Kvackaj (Ed.), Intech, Rijeka, Croatia (2011).
  20. C. Macchi, A. Tolley, R. Giovachini, I.J. Polmear, A. Somozo, Influence of a microalloying addition of Ag on the precipitation kinetics of an Al–Cu–Mg alloy with high Mg: Cu ratio. *Acta Mater.* **98**, 275–287 (2015). <https://doi.org/10.1016/j.actamat.2015.07.032>
  21. H.K. Hardy, The ageing characteristics of some ternary aluminium-copper-magnesium alloys with copper magnesium ratios of 71 and 221. *J. Ins. Met.* **83**, 17–34 (1954)
  22. I.J. Polmear, The effect of small additions of silver on the aging of some aluminium alloys. *Trans. Met. Soc. AIME* **230**, 1331–1339 (1964)
  23. S.P. Ringer, T. Sakurai, I.J. Polmear, Origins of hardening in aged Al–Cu–Mg–(Ag) alloys. *Acta Mater.* **45**, 3731–3744 (1997). [https://doi.org/10.1016/S1359-6454\(97\)00039-6](https://doi.org/10.1016/S1359-6454(97)00039-6)
  24. Q. Du, D.G. Eskin, L. Katgerman, Modeling macrosegregation during direct-chill casting of multicomponent aluminum alloys. *Metall. Mater. Trans.* **38**, 180–189 (2007). <https://doi.org/10.1007/s11661-006-9042-0>
  25. H. Wang, J. Xu, Y. Kang, M. Tang, Z. Zhang, Study on inhomogeneous characteristics and optimize homogenization treatment parameter for large size DC ingots of Al–Zn–Mg–Cu alloys. *J. Alloys Compd.* **585**, 19–24 (2014). <https://doi.org/10.1016/j.jallcom.2013.09.139>
  26. N. Nayan, S.Y.S.N. Murty-Gotvind, M.C. Mittal, P.P. Sinha, Optimization of homogenizing mode for aluminum alloy AA7075 using calorimetric and microstructural studies. *Met. Sci. Heat Treat.* **51**, 330 (2009). <https://doi.org/10.1007/s11041-009-9178-9>
  27. N. Gao, M.J. Starink, N. Kamp, I. Sinclair, Application of uniform design in optimisation of three stage ageing of Al–Cu–Mg alloys. *J. Mater. Sci.* **42**, 4398–4405 (2007). <https://doi.org/10.1007/s10853-006-0659-6>
  28. M. Zamani, S. Toschi, A. Morri, L. Ceschini, S. Seifeddine, Optimisation of heat treatment of Al–Cu–(Mg–Ag) cast alloys. *J. Therm. Anal. Calorim.* **139**, 3427–3440 (2020). <https://doi.org/10.1007/s10973-019-08702-x>
  29. W. Feng, Z. Yanqi, X. Baiqing, Z. Yongan, L. Xiwu, L. Zhihui, L. Hongwei, Effect of Si addition on microstructure and mechanical properties of Al–Cu–Mg alloy. *J. Alloys Compd.* **585**, 474–478 (2013). <https://doi.org/10.1016/j.jallcom.2013.08.214>
  30. R. Yamanoglu, E. Karakulak, A. Zeren, M. Zeren, Effect of heat treatment on the tribological properties of Al-Cu-Mg/nanoSiC composites. *Mater. Design.* **49**, 820–825 (2013). <https://doi.org/10.1016/j.matdes.2013.02.026>
  31. A.N. Petrova, H. Radziszewska, L. Kaczmarek, M. Klich, I.G. Brodova, M. Steglinski, Influence of megaplastic deformation on the structure and hardness of Al–Cu–Mg alloy after aging. *Phys. Met. Metallogr.* **117**, 1237–1244 (2016). <https://doi.org/10.1134/S0031918X16120103>
  32. A.M. Samuel, S.A. Alkahtani, H.W. Doty, F.H. Samuel, Role of Zr and Sc addition in controlling the microstructure and tensile properties of aluminum-copper based alloys. *Mater. Design.* **88**, 1134–1144 (2015). <https://doi.org/10.1016/j.matdes.2015.09.090>
  33. B. Zhao, Q. Cai, J. Cheng, S. Yang, F. Chen, Investigation on recrystallization and precipitation behaviors of Al–4.5Cu–1.5Mg alloy refined by Ti-supported TiC nanoparticles. *J. Alloys Compd.* **800**, 392–402 (2019). <https://doi.org/10.1016/j.jallcom.2019.05.323>
  34. J. Li, S. Chen, F. Li, K. Chen, L. Huang, Synergy effect of Si addition and pre-straining on microstructure and properties of Al–Cu–Mg alloys with a medium Cu/Mg ratio. *Mat. Sci. Eng. A* **767**, 138429 (2019). <https://doi.org/10.1016/j.msea.2019.138429>
  35. W.L. Zhang, D.H. Xiao, T. Li, J.D. Du, D.Y. Ding, Microstructure and mechanical properties of two-stage aged Al–Cu–Mg–Ag–Sm alloy. *Rare Met.* **38**, 42–51 (2019). <https://doi.org/10.1007/s12598-018-1137-4>
  36. J. Gu, M. Gao, S. Yang, J. Bai, Y. Zhai, J. Ding, Microstructure, defects, and mechanical properties of

- wire + arc additively manufactured Al–Cu4.3–Mg1.5 alloy. *Mater. Design.* **186**, 108357 (2020). <https://doi.org/10.1016/j.matdes.2019.108357>
37. S. Chen, K. Chen, G. Peng, L. Jia, P. Dong, Effect of heat treatment on strength, exfoliation corrosion and electrochemical behavior of 7085 aluminum alloy. *Mater. Design.* **35**, 93–98 (2012). <https://doi.org/10.1016/j.matdes.2011.09.033>
  38. L. Li, T.T. Zhou, H.X. Li, C.Q. Chen, B.Q. Xiong, L.K. Shi, Effect of additional elements on aging behavior of Al–Zn–Mg–Cu alloys by spray forming. *Trans. Nonferrous Met. Soc. China* **16**, 532–538 (2006). [https://doi.org/10.1016/S1003-6326\(06\)60093-9](https://doi.org/10.1016/S1003-6326(06)60093-9)
  39. M. Chemingui, M. Khitouni, K. Jozwiak, G. Mesmacque, A. Kolsi, Characterization of the mechanical properties changes in an Al–Zn–Mg alloy after a two-step ageing treatment at 70° and 135 °C. *Mater. Design.* **31**, 3134–3139 (2010). <https://doi.org/10.1016/j.matdes.2009.12.033>
  40. L. Zhan, X. Wu, X. Wang, Y. Yang, G. Liu, Y. Xu, Effect of process parameters on fatigue and fracture behavior of Al–Cu–Mg alloy after creep aging. *Metals* **8**, 298 (2018). <https://doi.org/10.3390/met8050298>
  41. J. Zhang, Y.N. Huang, C. Mao, P. Peng, Structural, elastic and electronic properties of  $\theta$ (Al<sub>2</sub>Cu) and S(Al<sub>2</sub>CuMg) strengthening precipitates in Al–Cu–Mg series alloys: first-principles calculations. *Solid State Commun.* **152**, 2100–2104 (2012). <https://doi.org/10.1016/j.ssc.2012.09.003>
  42. L. Kaczmarek, M. Stenglinski, H. Radziszewska, L. Kolodziejczyk, J. Sawicki, W. Szymanski, R. Atraszkiewicz, J. Swiniarski, Effect of double-phase segregations formed due to two-stage aging on the strength properties of alloy PN-EN 2024. *Met. Sci. Heat Treat.* **54**, 477–482 (2013). <https://doi.org/10.1007/s11041-013-9534-7>
  43. Z.Q. Li, X.R. Zhang, S.Y. Zhang, Z.H. Shen, Determination of the elastic constants of metal-matrix composites by a laser ultrasound technique. *Compos. Sci. Technol.* **61**, 1457–1463 (2001). [https://doi.org/10.1016/S0266-3538\(01\)00045-8](https://doi.org/10.1016/S0266-3538(01)00045-8)

**Publisher's Note** Springer Nature remains neutral with regard to jurisdictional claims in published maps and institutional affiliations.